Laboratory Evidence of Organic Peroxide and Peroxyhemiacetal Formation in the Aqeuous Phase and Implications for Aqueous OH

Y. B. Lim[1,*] and B. J. Turpin[2]

[1]{Department of Environmental Sciences, Rutgers University, New Brunswick, NJ, USA}

[2]{Department of Environmental Science and Engineering, University of North Carolina at Chapel Hill, Chapel Hill, NC, USA}

[*]{now at: Center for Environmental, Health and Welfare Research, Korea Institute of Science and Technology, Seoul, Republic of Korea}

Correspondence to: Y. B. Lim (ylim@kist.re.kr)

Abstract

Aqueous chemistry in atmospheric waters (e.g., cloud droplets or wet aerosols) is considered a potentially important atmospheric pathway to produce secondary organic aerosol (SOA_{aq}). Water-soluble organic compounds with small carbon numbers (C_2-C_3) are precursors for SOA_{aq} and products include organic acids, organic sulfates, and high molecular weight compounds/oligomers. Fenton reactions and the uptake of gas-phase OH radicals are considered to be the major oxidant sources for aqueous organic chemistry. However, the sources and availability of oxidants in atmospheric waters are not well understood. The degree to which OH is produced in the aqueous phase affects the balance of radical and non-radical aqueous chemistry, the properties of the resulting aerosol, and likely its atmospheric behavior.

This paper demonstrates organic peroxide formation during aqueous photooxidation of methylglyoxal using ultra high resolution Fourier Transform Ion Cyclotron Resonance electrospray ionization mass spectrometry (FTICR-MS). Organic peroxides are known to form through *gas-phase* oxidation of volatile organic compounds. They contribute secondary organic aerosol (SOA) formation directly by forming peroxyhemiacetals, and epoxides (i.e., IEPOX), and indirectly by enhancing gas-phase oxidation through OH recycling. We provide

1 simulation results of organic peroxide/peroxyhemiacetal formation in clouds and wet aerosols

2 and discuss organic peroxides as a source of condensed-phase OH radicals and as a

3 contributor to aqueous SOA.

4

1 Introduction

6 Secondary organic aerosol (SOA) is a major component of atmospheric fine particulate matter

7 [$PM_{2.5}$] (Zhang et al., 2007), contributes to adverse health, and affects climate by scattering

8 (Seinfeld and Pandis, 1998) and sometimes by absorbing solar radiation (e.g., "brown

9 carbon") (Andreae and Gelencser, 2006; Bones et al., 2010; Zhang et al., 2011). Although the

10 chemical and physical properties of aerosols are needed to predict effects, the properties of

11 SOA are poorly understood because SOA formation itself is poorly understood. Aqueous

12 chemistry in atmospheric waters (e.g., cloud droplets or wet aerosols) is a potentially

13 important pathway to produce SOA (SOA_{aq}; Blando and Turpin, 2000), and could be

14 comparable in magnitude to "traditional" SOA, formed via partitioning of semivolatile

15 organic products of gas-phase oxidation (SOA_{gas}) globally (Liu et al., 2012; Lin et al., 2012;

16 Henze et al., 2008) and in locations where relative humidity and aerosol hygroscopicity are

17 high (Carlton and Turpin, 2013; Carlton et al., 2008; Fu et al., 2008; Chen et al., 2007).

18 Because SOA_{aq} is formed from small water-soluble precursors with high O/C ratios, it forms

19 SOA (e.g., oligomers, organic salts) with high O/C ratios and may explain the highly

20 oxygenated nature of atmospheric organic aerosols, while SOA_{gas} is less oxygenated (Aiken et

21 al., 2008; Lim et al., 2010 and 2013).

22 OH radicals are important oxidants in clouds. In the high solute concentrations in wet

23 aerosols, however, besides OH radical reactions a more complex system of organic radical

24 and non-radical reactions occurs (Lim et al., 2010; McNeill et al., 2012; Ervens et al., 2014).

25 Thus, an understanding of the availability of OH radicals is important to assessing the relative

26 importance of radical and non-radical chemistry in aerosols. The uptake of gas-phase OH

27 radicals into atmospheric waters (Faust and Allen, 1993) and Fenton reactions in the

28 condensed/aqueous media (Arakaki and Faust, 1998) are considered the major oxidant

29 sources for aqueous organic chemistry. Oxidant sources in organic-containing cloud, fog and

30 aerosol waters and oxidant reactions with dissolved organic compounds have been

31 documented (Arakaki et al., 2013; Weller et al., 2014; Long et al., 2013). Depending on

sources of OH radicals, aqueous oxidation reactions could exhibit a surface area dependence (e.g., controlled by OH uptake), or a volume dependence (e.g., controlled by OH production through aqueous chemistry; Ervens et al., 2014). Herein, we explore the hypothesis that organic peroxides produce OH radicals within the atmospheric aqueous phase; we also demonstrate the formation of organic peroxides in the aqueous phase and their contribution to *condensed* phase chemistry.

Organic peroxides (herein particularly, organic hydroperoxides = ROOH) are known to play an important role in gas phase chemistry. They are commonly found in the atmosphere with mixing ratios of 0.1-1 ppb (Lee et al., 1993; De Serves et al., 1994; Sauer et al., 2001; Grossmann et al., 2003; Lee et al., 2000; Guo et al., 2014). They are known to form through gas-phase reactions of volatile organic compounds (VOCs) with OH radical, NO_3 radical and O_3 (Atkinson and Arey, 2003). While their chemistry is not fully understood, these atmospheric organic species are "key" to peroxy radical/NO_x chemistry (Dibble, 2007; Glowacki et al., 2012), lead to photochemical smog formation, important to the HO_x-NO_x-O_3 balance (Wennberg et al., 1998; Singh et al., 1995), contribute to O_3 formation or depletion in the upper troposphere, and form SOA (Tobias and Ziemann, 2000; Ehn et al., 2014). Organic peroxides (formed from gas-phase ozonolysis of monoterpenes, e.g., α- and β-pinenes) are major constituents of SOA (Docherty et al., 2005). Monoterpenes have a global emission second only to isoprene among non-methane VOCs and maybe the most efficient SOA_{gas} precursor class (Kanakidou et al., 2005). Organic peroxides contribute to organic aerosol by forming peroxyhemiacetal oligomers with atmospherically abundant organic carbonyls (e.g., aldehydes and ketones) via acid catalysis in aerosols (Tobias and Ziemann, 2000; Ziemann, 2002). In general, due to the characteristically weak O-O bonds of organic peroxides, the gas-phase decomposition of organic peroxides through photolysis or intermolecular radical reactions recycles OH radicals and can enhance gas-phase photooxidation of atmospheric organic compounds. Recent field studies demonstrate that gas-phase OH recycling enhances isoprene photooxidation (Paulot et al., 2009; Taraborrelli et al., 2012). And a recent lab study (Badali et al., 2015) demonstrates that OH radicals are photolytically formed from the solutions of SOA from terpene ozonolysis and OH formation is likely due to photolysis of organic peroxides.

Organic peroxides are known to be moderately water soluble (Henry's law constant up to 1000 M/atm). They are present in rainwater with concentrations of 0.1 - 10 μM (Lind et al.,

1986; Hellpointer and Gab, 1989; Liang et al., 2013), presumably by uptake from the gas phase. Badali et al. (2015) measured OH radical formation from photolysis of terpene-O_3 SOA solutions and organic peroxide standard solutions (t-butyl hydroperoxide and cumene hydroperoxide). However, photolysis of the terpene SOA generates twice as much OH as is generated from a comparable amount of organic peroxide alone (i.e., standards). Since there should exist plenty of aldehydes formed from ozone reactions, we argue that organic peroxides could also be formed in the SOA solution during the photolytic experiments. In this work, we show that organic peroxides are also produced from aqueous-phase OH oxidation. We identify organic peroxide products from methylglyoxal and acid catalyzed oligomers (i.e., peroxyhemiacetals formed with methylglyoxal) by ultra-high resolution mass spectrometry. We simulate organic peroxide and peroxyhemiacetal formation under atmospheric conditions and explore organic peroxide contributions to aqueous-phase OH production and to SOA_{aq} formation.

2   Experimental Section

2.1   Cuvette Chamber Reactions

Reactions of methylglyoxal with OH radicals in the aqueous phase were conducted in a cuvette chamber, which holds 10 cuvettes (3 mL each; Spectrocell) equidistant from a 254 nm Hg UV lamp (Strahler). Cuvettes were immersed in a water bath to maintain the temperature at 25 ^{o}C. In each cuvette, 10 mM of methylglyoxal (Sigma-Aldrich) was dissolved in 18 MΩ Mili-Q water. OH radicals (10^{-13}—10^{-12} M) were generated in each cuvette by photolysis of 20 mM of H_2O_2 (Sigma-Aldrich) with the rate constant of 5.58e-5 M s^{-1}. The H_2O_2 photolysis rate constant was determined from H_2O_2 + UV control experiments conducted in the same cuvette chamber as described previously (Tan et al., 2010) and corrected for light absorption by H_2O_2 (Lim et al., 2013). Liu et al. (2012) and Zhao et al. (2013) found that α-hydroperoxides can form when methylglyoxal reacts with hydrogen peroxide in the dark. However, this reaction cannot explain the formation of the identified peroxy hemiacetals in this work (PHA_1 and PHA_2) since the molecular weight of the α-hydroperoxide is different from those of R_1OOH and R_2OOH. Moreover, according to control experiments by Tan et al. (2010) methylglyoxal degradation is much slower with hydrogen peroxide in the dark than it is with hydrogen peroxide in the UV light. Therefore, we do not expect the formation of the α-hydroperoxide in our photooxidation experiment.

4

1   The OH radical concentrations were estimated via modeling (Lim et al., 2013). It should be

2   noted that using 20 mM of H_2O_2 and the 254 nm UV lamp was not intended to simulate

3   tropospheric photolysis, rather to provide a source of OH radicals. According to our previous

4   control experiments (i.e., methylglyoxal + UV; methylglyoxal + H_2O_2), small amounts of

5   pyruvic, acetic and formic acids form slowly in control experiments. However, dicarboxylic

6   acids, the major products, did not form in the absence of OH radicals (i.e., in control

7   experiments; Tan et al., 2010). Photooxidation of methylglyoxal was allowed to proceed for

8   1 hr. After being removed from the chamber, the cuvettes were kept frozen until analysis. No

9   catalase was added in order to preserve organic peroxide products.

10   **2.2   Organic Peroxide and Peroxyhemiacetal Analysis**

11   Ultra high resolution Fourier Transform Ion Cyclotron Resonance Electrospray Ionization

12   Mass Spectrometer (FTICR-MS; Thermo-Finnigan LTQ-XL, Woods Hole Oceanographic

13   Mass Spectrometer Facility) was used to determine the elemental composition of organic

14   products as described previously (Altieri et al., 2008; Tan et al., 2012). The capillary voltage

15   and a capillary temperature were -30.00V and 300 °C, respectively for negative mode

16   analyses. Positive mode analyses were conducted with a capillary voltage of 20.00 V and a

17   capillary temperature of 260 °C. Both FTICR-MS and FTICR-MS/MS were used to analyze

18   organic peroxide products from aqueous photooxidation of methylglyoxal and a standard

19   solution, which was prepared by adding 10 mM of tert-butyl hydroperoxide (Sigma-Aldrich)

20   and 10 mM of methylglyoxal (Sigma-Aldrich). These samples were diluted 100 fold with

21   water (by volume), and diluted again with methanol (MeOH) by 2 fold (by volume). Thus,

22   the mobile phase consisted of 50% water and 50% MeOH; 0.1% of formic acid (by volume)

23   was also added. These diluted samples were immediately introduced into the electrospray

24   ionization source by direct infusion at 5 μL/min. Photooxidation products of methylglyoxal

25   were expected in both negative and positive modes due to a carboxylic group (negative mode)

26   and a hydroxyl group (positive mode) in their structure (Table 1), whereas tert-butyl

27   hydroperoxide is found only in the positive mode.

28

29   **3   Organic Peroxide Chemistry**

30   We hypothesize that aqueous-phase OH radical reactions of methylglyoxal lead to organic

31   peroxide formation as shown in Figure 1.   OH radical reactions are initiated by H-atom

1   abstraction. Subsequent O_2 addition and HO_2 decomposition mainly lead to the formation of

2   pyruvic acid and acetic acid (Lim et al., 2013). Both pyruvic and acetic acid react further

3   with OH radicals and O_2, forming peroxy radicals (RO_2), which undergo bimolecular RO_2-

4   RO_2 reactions (Lim et al., 2013). However, substantial amounts of peroxy radicals could also

5   react with HO_2 forming organic peroxides (as indicated by a bold arrow) since HO_2 is a

6   common byproduct of aqueous photooxidation (Lim et al., 2010 and 2013) and is also water

7   soluble (Henry's law constant = 4e3 M/atm; this is ~ 100 times higher than that of OH

8   radicals).

9   We further expect organic peroxides to form peroxyhemiacetals with aldehydes via acid

10   catalysis in the aqueous phase (Figure 2A), as they do in dry aerosols (Tobias and Ziemann,

11   2000; Docherty et al., 2005). Below we document the formation of peroxyhemiacetals from a

12   commercially available organic peroxide, tert-butyl hydroperoxide and methylglyoxal in

13   aqueous solution (Figure 2B). Then we argue that organic peroxide products (R_1OOH and

14   R_2OOH in Figure 1) from the aqueous OH oxidation of methylglyoxal react further with

15   methylglyoxal in water to produce peroxyhemiacetals. Briefly, a carbonyl group (aldehyde)

16   in methylglyoxal is protonated by H^+, then a hydroperoxyl group (-OOH) attacks a protonated

17   carbonyl group forming peroxyhemiacetal. This peroxyhemiacetal chemistry is a well

18   established oligomerization mechanism for SOA from gas-phase ozone reactions of alkenes in

19   smog chamber studies (Tobias and Ziemann, 2000). In Tobias and Ziemann study, organic

20   peroxides are first formed in the gas phase and become particles through gas-particle

21   partitioning. Then organic peroxides form peroxyhemiacetals with by-product aldehydes

22   through acid-catalyzed heterogeneous reactions on the particle surface. In current study, the

23   detection of peroxyhemiacetals in our aqueous chemistry experiments (see below) provides

24   evidence for organic peroxide formation through aqueous photochemistry.

25

4   Results and Discussion

4.1   Standard Solution (Mixture of Methylglyoxal and t-Butyl Hydroperoxide)

28   FTICR-MS and FTICR-MS/MS analyses of the aqueous mixture of methylglyoxal and t-butyl

29   hydroperoxide show methylglyoxal (m/z^+ 127.03666, 145.04714 and 159.06278) and a

30   peroxyhemiacetal (PHA_{std}; m/z^+ 185.07797) in the positive mode (Figure 3). In a mobile

31   phase of 50% MeOH and 50% water, methylglyoxal undergoes hydration with water and

32   hemiacetal formation with MeOH, and is detected as a sodium adduct (i.e., m/z^+ 127.03666 =

1   [methylglyoxal + MeOH + Na]$^+$, m/z$^+$ 145.04714 = [methylglyoxal + H$_2$O + MeOH + Na]$^+$,

2   and m/z$^+$ 159.06278 = [methylglyoxal + 2MeOH + Na]$^+$). Methylglyoxal solvation with

3   MeOH was verified by FTICR-MS/MS (Figure 4). The fragments of m/z$^+$ 159.06278 are

4   m/z$^+$ 141.05203 (H$_2$O loss), m/z$^+$ 127.03668 (MeOH loss), and m/z$^+$ 95.01041 (another

5   MeOH loss). The ion m/z$^+$ 95.01041 is the sodium adduct to methylglyoxal (a theoretical

6   reading for [methylglyoxal + Na]$^+$ is m/z$^+$ 95.01090). We are confident that m/z$^+$ 159.06278 is

7   a double hemiacetal of methanol with methylglyoxal, not a cluster of methylglyoxal with two

8   methanol molecules by the water loss in Fig. 4 and examination of ESI-MS standard runs for

9   glyoxal and methylglyoxal in the water mobile phase with and without methanol (See

10   Supplementary Material Fig. S5). A sodium adduct is also expected for a peroxyhemiacetals,

11   and seen in Figure 3 as m/z$^+$ 185.07797 (= [PHA$_{std}$ + Na]$^+$). Details of FTICR-MS readings

12   and theoretical readings based on actual molecular/atomic masses are shown in Table 1.

13   The PHA$_{std}$ peak, m/z$^+$ 185.07802 (theoretical reading of [PHA$_{std}$ + Na]$^+$ = 185.07899) was

14   fragmented by infrared multiphoton dissociation (IRMPD). Major fragments (Figure. 5) are

15   m/z$^+$ 153.05228 (MeOH loss) and m/z$^+$ 95.01041 ([methylglyoxal + Na]$^+$). In electron

16   impact (hard ionization), fragmentation of organic peroxides results in the loss of HO$_2$

17   (Tobias and Ziemann, 2000; Docherty et al., 2005). However, O$_2$ loss is expected for soft

18   ionization, IRMPD fragmentation in FTICR-MS/MS (M. Soule and E. Kujawinski, personal

19   communication, 2013; Detailed discussion in Supplementary Material). In Figure 5, the ion

20   m/z$^+$ 81.06971 indicates the loss of O$_2$ from t-butyl hydroperoxide. We also observed the O$_2$

21   loss (m/z$^+$ 153.07158) from PHA$_{std}$. FTICR-MS/MS and theoretical readings are provided in

22   Table 2.

23   Note that no organic peroxide peak was observed in the standard solution (nor in

24   methylglyoxal + OH samples). This is not surprising because 1) high temperature of the

25   capillary in an electrospray chamber (~ 250 ^{o}C) is likely to decompose organic peroxides

26   (Kharasch et al., 1950; M. Soule and E. Kujawinski, personal communication, 2013); 2) in the

27   ESI method, it is difficult to ionize organic peroxides (Witkowski and Gierczak, 2013) and

28   organic peroxides react with methylglyoxal to form peroxyhemiacetals. These

29   peroxyhemiacetals are much more stable and lesser volatile than organic peroxides (Tobias

30   and Ziemann, 2000). These peroxyhemiacetal peaks (and fragments) appear in FTICR-MS

31   (and FTICR-MS/MS) analysis of standard solutions and samples (see below), providing

32   evidence for the presence (and formation) of organic peroxides from methylglyoxal + OH.

FTICR-MS/MS of peroxyhemiacetal peaks show corresponding organic peroxide fragments, methylglyoxal and other fragments as expected (Tobias and Ziemann, 2000; Docherty et al., 2005).

4.2   Aqueous Photooxidation Products of Methylglyoxal

A FTICR mass spectrum of an aqueous methylglyoxal solution exposed to OH radicals for 60 minutes is shown in Figure 6 (negative mode). Main photooxidation products (Tan et al., 2012; Lim et al., 2013) are seen at m/z$^-$ 87.00862 (pyruvic acid) and m/z$^-$ 177.04036 (2, 3-dimethyltartaric acid; structure shown in Figure 6). This spectrum also provides evidence for peroxyhemiacetal formation at m/z$^-$ 163.02392 (= [PHA$_1$ - H]$^-$) and m/z$^-$ 191.01998 (= [PHA$_2$ - H]$^-$) since these readings are very close to the theoretical readings, m/z$^-$ 163.02405 for PHA$_1$ and m/z$^-$ 191.01918 for PHA$_2$ (Table 1). Fragmentation of these peaks by FTICR-MS/MS supports their identification as peroxyhemiacetals. In Figure 7A, m/z$^-$ 131.01339 and m/z$^-$ 131.01585 result from the losses of MeOH and O$_2$, respectively, from PHA$_1$ at m/z$^-$ 163.02405 and m/z$^-$ 59.01377 results from the loss of O$_2$ from R$_1$OOH, which is the organic peroxide constituent of PHA$_1$. Similarly, in Figure 7B, m/z$^-$ 159.02946 (C6H7O5) results from the loss of O$_2$ from PHA$_2$ at m/z$^-$ 191.02000. m/z$^-$ 87.00832 results from the loss of O$_2$ from R$_2$OOH, which is the organic peroxide constituent of PHA$_2$. Note that m/z$^-$ 191.02000 is PHA$_2$ while m/z$^-$ 191.05540 is prominent as a parent ion. Due to the small intensity we were unable to isolate m/z$^-$ 191.02000 from m/z$^-$ 191.05540 for MS/MS analyses. Therefore, for the PHA$_2$ analysis, we cannot rule out the possibility that m/z$^-$ 59.01377 [R$_2$OOH – O$_2$] could be the fragment from m/z$^-$ 191.05540 [C7H11O6]$^-$. As was the case with the mixed peroxide-aldehyde standard, the organic peroxides themselves were not observed (see previous section). Detected and theoretical readings are provided in Table 2.

The FTICR-MS/MS was also conducted in the positive mode (Figure 8) for PHA$_1$ (m/z$^+$ 187.02069 in Figure 8A) and PHA$_2$ (m/z$^+$ 215.01565 in Figure 8B). The theoretical readings are 187.02186 for PHA$_1$ and 215.01678 for PHA$_2$ (Table 1). The methylglyoxal fragments (m/z$^+$ 95.1041 in Figure 8A and m/z$^+$ 95.0140 in Figure 8B) appear. This confirms that both PHA$_1$ and PHA$_2$ are indeed acid-catalyzed products of methylglyoxal. Note that for the PHA$_2$ analysis in the positive mode, again, we cannot rule out the possibility that methylglyoxal [m/z$^+$ 95.01040] could be the fragment of m/z 215.05151 [C7H12O6Na]$^+$.

5 Atmospheric Implications

Using ultra-high resolution FTICR-MS and FTICR-MS/MS, we observed the presence of peroxyhemiacetals, after aqueous photooxidation of methylglyoxal and in aqueous methylglyoxal-organic peroxide standard solutions. The presence of stable peroxyhemiacetals is an indicator of the existence of the less stable organic peroxides. Thus, this work provides evidence for the formation of organic peroxides through aqueous phase OH radical oxidation of methylglyoxal.

5.1 Organic Peroxide Production in Clouds and Wet Aerosols

Below we demonstrate through chemical modeling that organic peroxides photochemically form from organics present both in clouds and wet aerosols. We used the full kinetic model for glyoxal and methylglyoxal (Lim et al., 2013) to simulate the formation of organic peroxides and peroxyhemiacetals. The following updates were made to the model: 1) The rate constant for the bimolecular reactions of RO_2 and HO_2 was given as 3e6 $M^{-1}s^{-1}$ (Reaction 213-219 in Table S1) based on the rate constant for [$HO_2 + HO_2$] ~ 1e6 $M^{-1}s^{-1}$; 2) The concentration of OH in the aqueous phase was set to ~ 10^{-14} (previously ~10^{-12}) according to recent estimations (Arakaki et al., 2013) (Figure S1A); 3) The concentration of HO_2 photochemically formed in the aqueous phase was estimated to be ~ 10^{-8} M maintained by the Henry's law equilibrium; therefore, the excess HO_2 produced by photooxidation in the aqueous phase was transported to the gas phase (Figure S1B). All the reactions included in the model are listed in Table S1.

For wet aerosol simulations, 1 M (the initial concentration) of methylglyoxal was used in the aqueous phase. Note that we do not expect that methylglyoxal is present at 1 M in aerosols. However, water-soluble organic matter is present at 1-10 M. So this analysis treats all water-soluble organic matter as if it behaves like methylglyoxal. Under wet aerosol conditions ([methylglyoxal]$_{initial}$ = 1 M, [H_2O_2]$_{initial}$ = 0 M, [OH] ~ 10^{-14} M, and [HO_2] ~ 10^{-8} M), ~ 400 µM of organic peroxides during the 12-hr daytime were formed through aqueous OH radical reactions (Figure 10A). The model also includes the sinks of aqueous-phase organic peroxides: OH radical reactions (R220-225), photolysis (R230), and the evaporation to the gas phase (R234) in Table S1. Note that organic peroxide (ROOH) formation in Figure 10A and B does not change within the Henry's law constant, 100 to 1000 M/atm, and the evaporation rate is assumed to be a diffusion-controlled transfer coefficient (Lelieveld and Crutzen, 1991;

1   Lim et al., 2005), which is the upper limit based on the equation provided by Lelieveld and

2   Crutzen (1991). Here, the gas-phase [ROOH] is assumed to be 1 ppb (R234 in Table S1).

3   In atmospheric cloud conditions ([methylglyoxal]$_{initial}$ = 10 µM, [H$_2$O$_2$]$_{initial}$ = 0 M, [OH] ~ 10^{-}

4   ^{14} M, and [HO$_2$] ~ 10^{-8} M), ~ 0.4 µM of organic peroxide formation during the 12-hr daytime

5   is expected (Figure 10B) while all the sinks of organic peroxides listed above are included.

6   This concentration of aqueous-phase photochemically produced organic peroxides is within

7   the range of measured rainwater concentrations (0.1 – 10 µM) and similar to the concentration

8   expected by Henry's law equilibrium from gas-phase organic peroxides (0.1 – 1 ppb).

9   **5.2   Peroxyhemiacetal Formation in Wet Aerosol**

10   The formation of peroxyhemiacetals competes with 1) hydration of methylglyoxal and 2)

11   photolysis and OH reactions of organic peroxides (Figure 9). Competing with methylglyoxal

12   hydration means that only a dehydrated methylglyoxal (DeMGLY), not hydrated

13   methylglyoxal (MGLY), forms a peroxyhemiacetal (PHA) with an organic peroxide (ROOH),

14   since the aldehyde reacts with peroxides. The dehydration equilibrium for methylglyoxal is

15   included in the model (R226 in Table S1). In wet aerosols, ~ 0.4 mM of DeMGLY out of 1 M

16   MGLY will undergo peroxyhemiacetal formation and react with OH radicals (R227 and R228

17   in Table S1) at the same time (Figure S2A). The main sink for peroxyhemiacetals is expected

18   to be OH reaction (no evaporation is expected). The peroxyhemiacetal formation equilibrium

19   (R229) and the OH reaction of peroxyhemiacetals (R231) are listed in Table S1.   The

20   modified model simulates ~ 0.4 µM of peroxyhemiacetal formation during the 12-hr daytime

21   and the minor increase during the nighttime (Figure 10A).   Under cloud conditions,

22   peroxyhemiacetal formation is negligible (Note that the model simulates ~ 4e-15 M

23   peroxyhemiacetal formation during the daytime from 10 µM of methylglyoxal photooxidation

24   in Figure 10B).

25   **5.3   OH Recycling Due to the Photolysis of Organic Peroxides in Atmospheric**

26   **Waters**

27   In both cloud and wet aerosol conditions, 7.5e-15 M of aqueous-phase OH production is

28   expected from the photolysis of organic peroxides ([ROOH]$_{initial}$ ~ 400 µM in wet aerosols

29   and [ROOH]$_{initial}$ ~ 0.4 µM in cloud droplets) formed by aqueous photooxidation during the

30   12-hr daytime (Figure S3) while the sink of ROOH is OH reaction. Note that Badali et al.

31   (2015) confirmed OH formation from photolysis of solutions of organic peroxide SOA and

measured OH formation rates are comparable to an estimation by Arakaki et al. (2013), which is $\sim 10^{-14}$ M OH in atmospheric waters, and $\sim 10^{-14} - 10^{-15}$ M of OH was previously estimated in the core of the bulk phase (Jacob 1986). Thus, the aqueous production of organic peroxides in atmospheric waters could be an important source of aqueous OH through organic peroxide photolysis.

References

Aiken, A. C., DeCarlo, P. F., Kroll, J. H., Worsnop, D. R., Huffman, J. A., Docherty, K.,Ulbrich, I. M., Mohr, C., Kimmel, J. R., Sueper, D., Zhang, Q., Sun, Y., Trimborn, A.,Northway, M., Ziemann, P. J., Canagaratna, M. R., Onasch, T. B., Alfarra, R., Prevot, A. S. H., Dommen, J., Duplissy, J., Metzger, A., Baltensperger, U., and Jimenez, J. L.: O/C and OM/OC Ratios of Primary, Secondary, and Ambient Organic Aerosols with High Resolution Time-of-Flight Aerosol Mass Spectrometry, Environ. Sci. Technol., 42, 4478-4485, 2008.

Altieri, K. E., Seitzinger, S. P., Carlton, A. G., Turpin, B. J., Klein, G. C., and Marshall, A. G.: Oligomers Formed through In-Cloud Methylglyoxal Reactions: Chemical Composition, Properties, and Mechanisms Investigated by Ultra-High Resolution FT-ICR Mass Spectrometry, Atmos. Environ., 42, 1476-1490, 2008.

Andreae, M. O. and Gelencser, A.: Black Carbon or Brown Carbon? The Nature of Light-Absorbing Carbonaceous Aerosols, Atmos. Chem. Phys., 6, 3131-3148, 2006.

Arakaki, T. and Faust, B. C.: Sources, Sinks, and Mechanisms of Hydroxyl Radical (OH) Photoproduction and Consumption in Authentic Acidic Continental Cloud Waters From Whiteface Mountain, New York: The Role of the Fe(R) (R = II, III) Photochemical Cycle, J. Geophys. Res. 103(D3), 3487-3504, 1998.

Arakaki, T., Anastasio, C., Kuroki, Y., Nakjima, H., Okada, K., Kotani, Y., Handa, D., Azechi, S., Kimura, T., Tsuhako, A., and Miyagi, Y.: A General Scavenging Rate Constant for Reaction of Hydroxyl Radical with Organic Carbon in Atmospheric Waters, Environ. Sci. Technol., 47, 8196-8203, 2013.

Atkinson, R., and Arey, J.: Atmospheric Degradation of Volatile Organic Compounds, Chem. Rev., 103, 4605-4638, 2003.

Badali, K. M., Zhou, S., Aljawhary, D., Antinolo, M., Chen, W. J., Lok, A., Mungall, E., Wong, J. P. S., Zhao, R., and Abbatt, J. P. D.: Formation of Hydroxyl Radicals from Photolysis of Secondary Organic Aerosol Material, Atmos. Chem. Phys., 15, 7831-7840, 2015.

Blando, J. D. and Turpin B. J.: Secondary Organic Aerosol Formation in Cloud and Fog Droplets: A Literature Evaluation of Plausibility, Atmos. Environ., 34, 1623-1632, 2000.

Bones, D. L., Henricksen, D. K., Mang S. A., Gonsior, M., Bateman, A. P., Nguyen, T. B., Cooper, W. J., and Nizkorodov, S. A.: Appearance of Strong Absorbers and Fluorophores in Limonene-O_3 Secondary Organic Aerosol Due to NH4+-Mediated Chemical Aging Over Long Time Scales, J. Geophysical Res., 115, D05203, doi:10.1029/2009JD01864, 2010.

Carton, A. G. Turpin, B. J., Altieri, K. E., Seitizinger, S. P., Mathur, R., Roselle, S. J., and Weber, R. J.: CMAQ Model Performance Enhanced When In-Cloud Secondary Organic Aerosol is Included: Comparisons of Organic Carbon Predictions with Measurements, Environ. Sci. Technol., 42, 8798-8802, 2008.

Carlton, A. G., and Turpin, B. J.: Particle Partitioning Potential of Organic Compounds is Highest in the Eastern US and Driven by Anthropogenic Water, Atmos. Chem. Phys., 13, 10203-10214, doi:10.5194/acp-13-13203-2013, 2013.

Chen, J., Griffin, R. J., Grini, A., and Tulet, P.: Modeling Secondary Organic Aerosol Formation Through Cloud Processing of Organic Compounds, Atmos. Chem. Phys., 7, 5343-5355, 2007.

De Serves, C.: Gas Phase Formaldehyde and Peroxide Measurements in the Artic Atmosphere, J. Geophys. Res., 99, 5471-5483, 1994.

Dibble, T. S. Failures and Limitations of Quantum Chemistry for Two Key Problems in the Atmospheric Chemistry of Peroxy Radicals, Atmos. Environ., 42, 5837-5848, 2007.

Docherty, K. S., Wu, W., Lim, Y. B., and Ziemann, P. J.: Contribution of Organic Peroxides to Secondary Organic Aerosol Formed from Reactions of Monoterpenes with O_3, Environ. Sci. Technol., 39, 4049-4059, 2005.

Ehn, M., Thornton, J. A., Kleist, E., Sipila, M., Junninen, H., Pullinen, I., Springer, M., Rubach, F., Tillmann, R., Lee, B., Lopez-Hilfiker, F., Andres, S., Acir, I., Rissanen, M., Jokinen, T., Schobesberger, S., Kangasluoma, J., Kontkanen, J., Nieminen, T., Kurten, T., Nielsen, L., Jorgensen, S., Kjaegaard, H. G., Canagaratna, M., Maso, M. D., Berndt, T., Petaja, T., Wahner, A., Kerminen, V., Kulmala, M., Worsnop, D. R., Wildt, J., and Mentel, F.: A Large Source of Low-Volatility Secondary Organic Aerosol, Nature, 506, 476-479, 2014.

Ervens, B., Sorooshian, A., Lim, Y. B., Turpin, B. J.: Key Parameters Controlling OH-Initiated Formation of Secondary Organoc Aerosol in the Aqueous Phase (aqSOA), J. Geophys. Res. Atmos., 119, 3997-4016, 2014.

1   Faust, B. C. and Allen, J. M.: Aqueous-Phase Photochemical Formation of Hydroxyl Radical
2   in Authentic Cloudwaters and Fogwaters, Environ. Sci. Technol., 27, 1221-1224, 1993.

3   Fu, T-M., Jacob, D. J., Wittrock, F., Burrows, J. P., Vrekoussis, M. and Henze, D. K. Global
4   Budgets of Atmospheric Glyoxal and Methylglyoxal, and Implications for Formation of
5   Secondary Organic Aerosols, J. Geophys. Res., 113, D15303, doi:10.1029/2007JD009505,
6   2008.

7   Glowacki, D. R., Lockhart, J., Blitz, M. A., Klippenstein, S. J., Piling, M. J., Robertson, S. H.,
8   and Seakins, P. W.: Interception of Excited Vibrational Quantum States by O2 in
9   Atmospheric Association Reactions, Science, 337, 1066-1069, 2012.

10 Grossmann, D., Moortgat, G. K., Kibler, M., Schlomski, S., Bachmann, K., Alicke, B., Geyer,
11 A., Platt, U., Hammer, M.-U., and Vogel, B.: Hydrogen Peroxide, Organic Peroxides,
12 Carbonyl Compounds and Organic Acids Measured at Pabstthum during BERLIOZ, J.
13 Geophys. Res. 108, doi:10.1029-2001JD001096, 2003.

14 Guo, J., Tilgner, A., Yeung, C., Wang, Z., Louie, P. K. K., Luk, C. W. Y., Xu, Z., Yuan, C.,
15 Gao, Y., Poon, S., Herrmann, H., Lee, S., Lam, K. S., and Wang, T.: Atmospheric Peroxides
16 in a Polluted Subtropical Environment: Seasonal Variation, Sources and Sinks, and
17 Importance of Heterogeneous Processes, Environ. Sci. Technol., 48, 1443-1460, 2014.

18 Hellpointer E. and Gab, S.: Detection of Methyl, Hydroxymethyl and Hydroxyethyl
19 Hydroperoxides in air and precipitation, Nature, 337, 631-634, 1989.

20 Henze, D. K., Seinfeld, J. H., Ng, N. L., Kroll, J. H., Fu, T-M., Jacob, D. J., and Heald, C. L.:
21 Global Modeling of Secondary Organic Aerosol Formation from Aromatic Hydrocarbons:
22 High- vs. Low-Yield Pathways, Atmos. Chem. Phys., 8, 2405-2420, 2008.

23 Jacob, D. J.: Chemistry of OH in Remote Clouds and Its Role in the Production of Formic
24 Acid and Peroxymonosulfate, J. Geophys. Res. 91(D9), 9807-9826, 1986.

25 Kanakidou, M., Seinfeld, J. H., Pandis, S. N., Barnes, I., Dentener, F. J., Facchini, M. C., Van
26 Dingenen, R., Ervens, B., Nenes, A., Nielsen, C. J., Swietlicki, E., Putaud, J. P., Balkanski,
27 Y., Fuzzi, S., Horth, J., Moortgat, G. K., Winterhalter, R., Myhre, C. E. L., Tsigaridis, K.,
28 Vignati, E., Stephanou, E. G., and Wilson, J.: Organic Aerosol and Global Climate
29 Modelling: a Review, Atmos. Chem. Phys., 5, 1053-1123, 2005.

Kharasch, M. S., Fono, A., and Nudenberg, W.: The Chemistry o Hydroperoxides. VI. The Thermal Decomposition of α-Cumyl Hydroperoxide, J. Org. Chem., 15, 748-752, 1950.

Lee, J. H., Leahy, D. F., Tang, I. N. and Newman, L. Measurement and Speciation of Gas-Phase Peroxides in the Atmosphere, J. Geophys. Res., 98, 2911-2915, 1993.

Lee, M., Heikes, B. G. and O'Sullivan, D. W.: Hydrogen Peroxide and Organic Hydroperoxide in the Troposphere: a Review, Atmos. Environ., 34:3475-3494, 2000.

Lelieveld, J. and Crutzen, P. J.: The Role of Clouds in Tropospheric Photochemistry, J. Atmos. Chem., 12, 229-267, 1991.

Liang, H., Chen, Z. M., Huang, D., Zhao, Y., and Li, Z. Y.: Impacts of Aerosols on the Chemistry of Atmospheric Trace Gases: A Case Study of Peroxides and HO_2 Radicals, Atmos. Chem. Phys., 13, 11259-11276, 2013.

Lim, H. J., Carlton, A. G., and Turpin, B. J.: Isoprene forms secondary organic aerosol through cloud processing: model simulations, Environ. Sci. Tech., 39, 4441-4446, 2005.

Lim, Y. B., Tan, Y., Perri, M., Seitzinger, S. P., and Turpin, B. J.: Aqueous Chemistry and Its Role in Secondary Organic Aerosol (SOA) Formation, Atmos. Chem. Phys., 10, 10521-10539, 2010.

Lim, Y. B., Tan, Y., and Turpin, B., J.: Chemical Insights, Explicit Chemistry, and Yields of Secondary Organic Aerosol from OH Radical Oxidation of Methylglyoxal and Glyoxal in the Aqueous Phase, Atmos. Chem. Phys., 13, 8651-8667, 2013.

Lin, G., Penner, J. E., Sillman, S., Taraborrelli, D., and Lelieveld, J.: Global Modeling of SOA Formation from Dicarbonyls, Epoxides, Organic Nitrates and Peroxides, Atmos. Chem. Phys., 12, 4743-4774, 2012.

Lind, J. A. and Kok, G.: Henry's Law Determinations for Aqueous Solutions of Hydrogen Peroxide, Methylhydroperoxide, and Peroxyacetic Acid, J. Geophys. Res., 91, 7889-7895, 1986.

Liu, J., Horowitz, L. W., Fan, S., Carlton, A. G., and Levy II, H.: Global In-Cloud Production of Secondary Organic Aerosols: Implementation of a Detailed Chemical in the GFDL Atmospheric Model AM3, J. Geophys. Res., 117, D15303, doi:10.1029/2012JD017838. 2012a.

Liu, Y., Monod, A., Tritscher, T., Praplan, A. P., DeCarlo, P. F., Temime-Roussel, B., Quivet, E., Marchand, N., Dommen, J., and Baltensperger, U: Aqueous Phase Processing of Secondary Organic Aerosol from Isoprene Photooxidation, Atmos. Chem. Phys., 12, 5879-5895, 2012b.

Long, Y., Charbouillot, T., Brigante, M., Maihot, G., Delort, A-M., Chaumerliac, N., and and Deguillaume, L.: Evaluation of Modeled Cloud Chemistry Mechanism against Laboratory Irradiation Experiments: The HxOx/Iron/Carboxylic Acid Chemical System, Atmos. Environ., 77, 686-695, 2013.

McNeill, V. F., Woo, J. L., Kim, D. D., Schwier, A. N., Wannell, N. J., Sumner, A. J., Barakt, J. M.: Aqueous-Phase Secondary Organic Aerosol and Organosulfate Formation in Atmospheric Aerosols: A Modeling Study, Environ. Sci. Technol., 46, 8075-8081, 2012.

Paulot, F., Crounse, J. D., Kjaergaard, H. G., Kurten, A., Clair, J. M. St., Seinfeld, J. H., and Wennberg, P. O.: Unexpected Epoxide Formation in the Gas-Phase Photooxidation of Isoprene, Science, 325, 730-733, 2009.

Sauer, F., Beck, J., Schuster, G. and Moortgat, G. K.: Hydrogen Peroxide, Organic Peroxides and Organic Acids in a Forest Area During FIELDVOC'94, Chemosphere Global Change Sci., 3, 309-326, 2001,

Seinfeld, J. H., and Pandis, S. N.: *Atmospheric Chemistry and Physics*, First Edition, Wiley-Interscience, New York, 1998.

Seinfeld, J. H., and Pankow, J. F.: Organic Atmospheric Particulate Material, Ann. Rev. Phys. Chem., 54, 121-140, 2003.

Singh, Hanwant, Kanakidou, M., Crutzen, P. J., and Jacob, D. J.: High Concentrations and photochemical fate of oxygenated hydrocarbons in the global troposphere, Nature, 2, 50-54. 1995.

Tan, Y., Carlton, A. G., Seitzinger, S. P., and Turpin, B. J.: SOA from methylglyoxal in clouds and wet aerosols: measurements and prediction of key products, Atmos. Environ., 44, 5218-5226, 2010.

Tan, Y., Lim, Y. B., Altieri, K. E., Seitzinger, S. P. and Turpin, B. J.: Mechanisms leading to oligomers and SOA through aqueous photooxidation: insights from OH radical oxidation of

acetic acid and methylglyoxal, Atmos. Chem. Phys., 12, 801-813, doi:10.5194/acp-12-801-2012, 2012.

Taraborrelli, D., Lawrence, M. G., Crowley, J. N., Dillon, T. J., Gromov, S., Groβ, C. B. M., Vereecken, L., and Lelieveld, J.: Hydroxyl Radical Buffered by Isoprene Oxidation over Tropical Forests, Nature Geosci., 5, 190-193, 2012.

Tobias, H. J., and Ziemann, P. J.: Thermal Desorption Mass Spectrometric Analysis of Organic Aerosol Formed from Reactions of 1-Tetradecene and O_3 in the Presence of Alcohols and Carboyxlic Acids, Environ. Sci. Technol., 34, 2105-2115, 2000.

Weller, C., Tilgner, A., Brauer, P., and Herrmann, H.: Modeling the Impact of Iron-Carboxylate Photochemistry on Radical Budget and Carboxylate Degradation in Cloud Droplet and Particles, Environ. Sci. Technol., 48, 5652-5659, 2014.

Wennberg, P. O., Hanisco, T. F., Jaegle, L., Jacob, D. J., Histsa, E. J., Lanzendorf, E. J., Anderson, J. G., Gao, R.-S., Kelm E. R., Donnelly, S. G., Del Negro, L. A., Fahey, D. W., McKeen, S. A., Salawitch, R. J., Webster, C. R., May, R. D., Herman, R. L., Proffit, M. H., Margitan, J. J., Atlas, E. L., Schauffler, S. M., Flocke, F., EmElroy, C. T., and Bui, T. P.: Hydrogen Radicals, Nitrogen Radicals, and the Production of O_3 in the Upper Troposphere, Science, 279, 49-53, 1998.

Witkowski, B. and Gierczak, T.: Analysis of α-Acyloxyhydroperoxy Aldehydes with Electrospray Ionization-Tandem Mass Spectrometry (ESI-MS^n), J. Mass Spectrom., 48, 79-88, 2013.

Zhang, Q., Jimenez, J. L., Canagaratna, M. R., Allan, J. D., Coe, H., Ulbrich, I., Alfarra, M. R., Takami, A., Middlebrook, A. M., Sun, Y. L., Dzepina, K., Dunlea, E., Docherty, K., DeCarlo, P. F., Salcedo, D., Onasch, T., Jayne, J. T., Miyoshi, T., Shimono, A., Hatakeyama, S., Takegawa, N., Kondo, Y., Schneider, J., Drewnick, F., Weimer, S., Demerjian, K., Williams, P., Bower, K., Bahreini, R., Cottrell, L., Griffin, R. J., Rautiainen, J., and Worsnop, D. R.: Ubiquity and Dominance of Oxygenated Species in Organic Aerosols in Anthropogenically-Influenced Northern Hemisphere Mid-Latitudes, Geophys. Res. Lett., 34, L13801, doi:10.1029/2007GL029979, 2007.

Zhang, X., Lin, Y. –H, Surratt, J. D., Zotter, P., Prevot, A. H. S., and Weber, R. J.: Light-Absorbing Soluble Organic Aerosol in Los Angeles and Atlanta: A Contrast in Secondary Organic Aerosol, Geophys. Res. Lett., 38, L21810, doi:10.1029/2011GL049385, 2011.

1   Zhao, R., Lee, A. K. Y., Soong, R., Simpson, A. J., and Abbatt, J. P. D.: Formation of

2   Aqueous-Phase α-Hydroxyhydroperoxides (α-HHP): Potential Atmospheric Impacts, Atmos.

3   Chem. Phys., 13, 5857-5872, 2013.

4   Ziemann, P. J.: Evidence of Low-Volatility Diacyl Peroxides as a Nucleating Agent and

5   Major Component of Aerosol Formed from Reactions of O_3 with Cyclohexene and

6   Homologous Compounds, J. Phys. Chem. A, 106, 4390-4402, 2002.

7

TABLE 1. FTICR-MS and theoretical readings for methylglyoxal, organic peroxides and peroxy hemicetals.

Methylglyoxal		Organic Peroxide		Peroxyhemiacetal (= Methylglyoxal + Organic Peroxide)	
(structure: methylglyoxal)		(structure: t-butyl hydroperoxide)		(structure: PHA$_{std}$)	
MW 72.02113		MW 90.06809		MW 162.08922	
Theoretical Reading[a]	**FTICR-MS Reading**	**Theoretical Reading[a]**	**FTICR-MS Reading**	**Theoretical Reading[a]**	**FTICR-MS Reading**
(structure)[c] MeO / HO / O $[M + MeOH^{b} + Na]^{+}$ = 127.03715	m/z^{+} 127.03666	$[M + Na]^{+}$ = 113.05786	m/z^{+} (Not Detected)	$[M + Na]^{+}$ = 185.07899	m/z^{+} 185.07797
		(structure: R$_1$OOH)		(structure: PHA$_1$)	
		MW 92.01096		MW 164.03209	
		Theoretical Reading[a]	**FTICR-MS Reading**	**Theoretical Reading[a]**	**FTICR-MS Reading**
(structure)[c] MeO / HO / OH / OH $[M + H_2O + MeOH^{b} + Na]^{+}$ = 145.04768	m/z^{+} 145.04714	$[M - H]^{-}$ = 91.00314	m/z^{-} (Not Detected)	$[M - H]^{-}$ = 163.02427 $[M + Na]^{+}$ = 187.02186	m/z^{-} 163.02405 m/z^{+} 187.02069
		(structure: R$_2$OOH)		(structure: PHA$_2$)	
		MW 120.00588		MW 192.02701	
(structure)[c] MeO / HO / OH / OMe [c] $[M + 2MeOH^{b} + Na]^{+}$ = 159.06330	m/z^{+} 159.06278	**Theoretical Reading[a]**	**FTICR-MS Reading**	**Theoretical Reading[a]**	**FTICR-MS Reading**
		$[M - H]^{-}$ = 118.99805	m/z^{-} (Not Detected)	$[M - H]^{-}$ = 191.01918 $[M + Na]^{+}$ = 215.01678	m/z^{-} 191.01998 m/z^{+} 215.01565

[a]Theoretical reading is based on actual atomic/molecular weights obtained by online software,
"Molecular Isotopic Distribution Analysis (MIDAs)"
(http://www.ncbi.nlm.nih.gov/CBBresearch/Yu/midas/index.html).
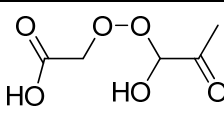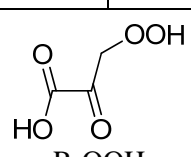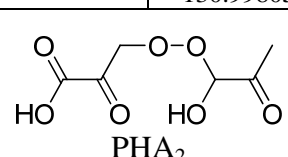[b]MeOH = Methanol. Note that the mobile phase contains 50% water (with 0.05% formic acid) and
50% MeOH.
[c]MeO is a deprotonated MeOH.
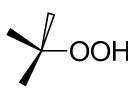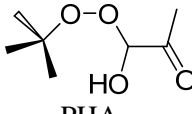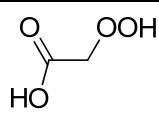
1 TABLE 2. FTICR-MS/MS and theoretical readings for fragments of peroxyhemiacetals and
2 organic peroxides
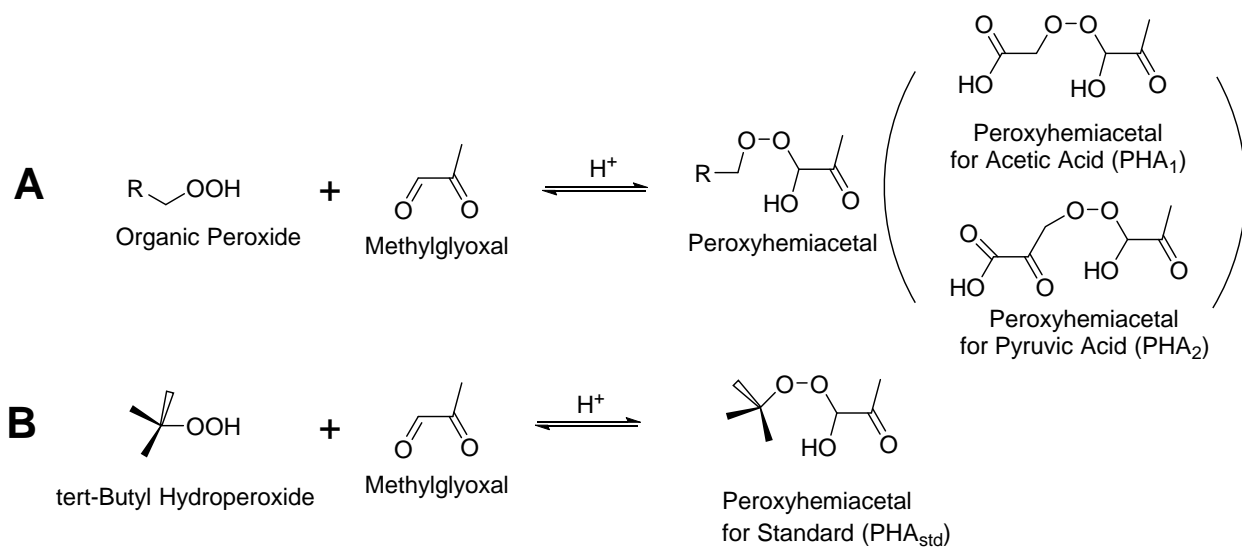
| Organic Peroxide			Peroxyhemiacetal		
t-butyl hydroperoxide			PHA$_{std}$		
Fragment (loss of O$_2$)		Fragment (loss of O$_2$)		Fragment (loss of MeOH)	
Theoretical Reading	FTICR-MS/MS Reading	Theoretical Reading	FTICR-MS/MS Reading	Theoretical Reading	FTICR-MS/MS Reading
$[M + Na - O_2]^+ =$ 81.06803	m/z$^+$ 81.06971	$[M + Na - O_2]^+ =$ 153.08916	m/z$^+$ 153.07158	$[M + Na - MeOH]^+ =$ 153.05277	m/z$^+$ 153.05228
R$_1$OOH			PHA$_1$		
Fragment (loss of O$_2$)		Fragment (loss of O$_2$)		Fragment (loss of MeOH)	
Theoretical Reading	FTICR-MS/MS Reading	Theoretical Reading	FTICR-MS/MS Reading	Theoretical Reading	FTICR-MS/MS Reading
$[M - H - O_2]^- =$ 59.01331	m/z$^-$ 59.01377	$[M - H - O_2]^- =$ 131.03444	m/z$^-$ 131.01589	$[M - H - MeOH]^- =$ 130.99805	m/z$^-$ 131.01339
R$_2$OOH			PHA$_2$		
Fragment (loss of O$_2$)		Fragment (loss of O$_2$)		Fragment (loss of MeOH)	
Theoretical Reading	FTICR-MS/MS Reading	Theoretical Reading	FTICR-MS/MS Reading	Theoretical Reading	FTICR-MS/MS Reading
$[M - H - O_2]^- =$ 87.00822	m/z$^-$ 87.00832	$[M - H - O_2]^- =$ 159.02935[e]	m/z$^-$ 159.02946	$[M - H - MeOH]^- =$ 159.00079	m/z$^-$ (Not Detected)

3
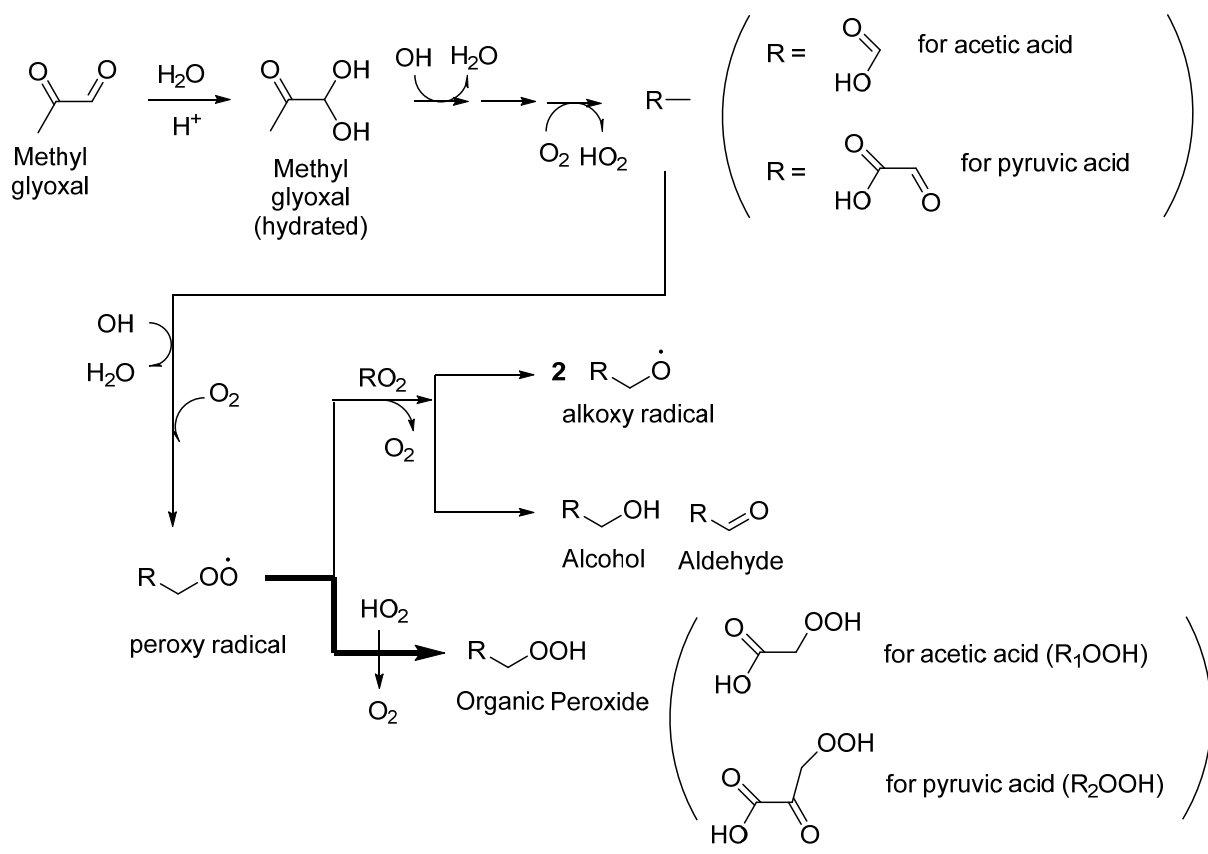
1

2   Figure 1. Organic peroxide formation from aqueous-phase OH radical reactions of
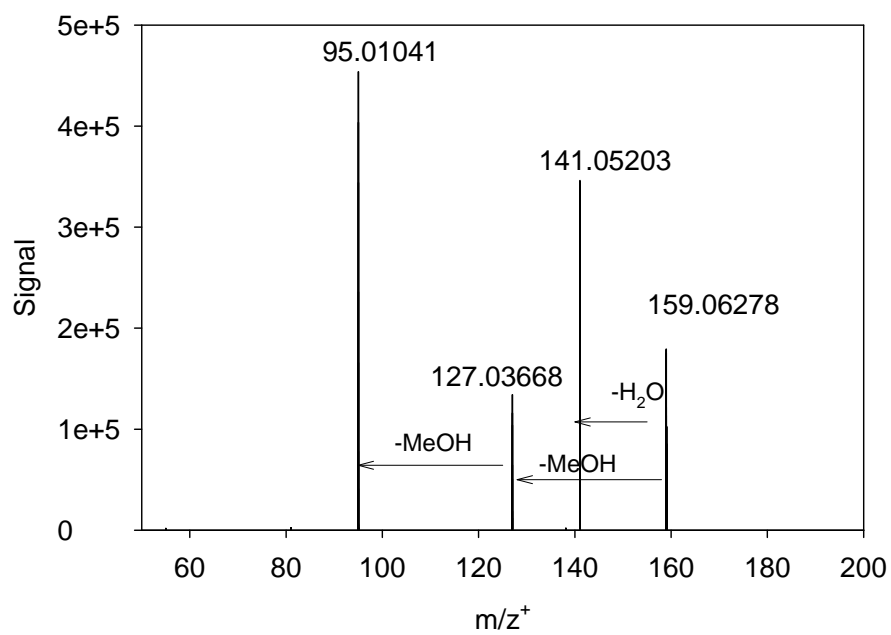
3   methylglyoxal.

Figure 2. Acid-catalyzed peroxyhemiacetal formation from a precursor, methylglyoxal with organic peroxide products of aqueous photooxidation (A) and from methylglyoxal with tert-butyl hydroperoxide in standard solutions (B).
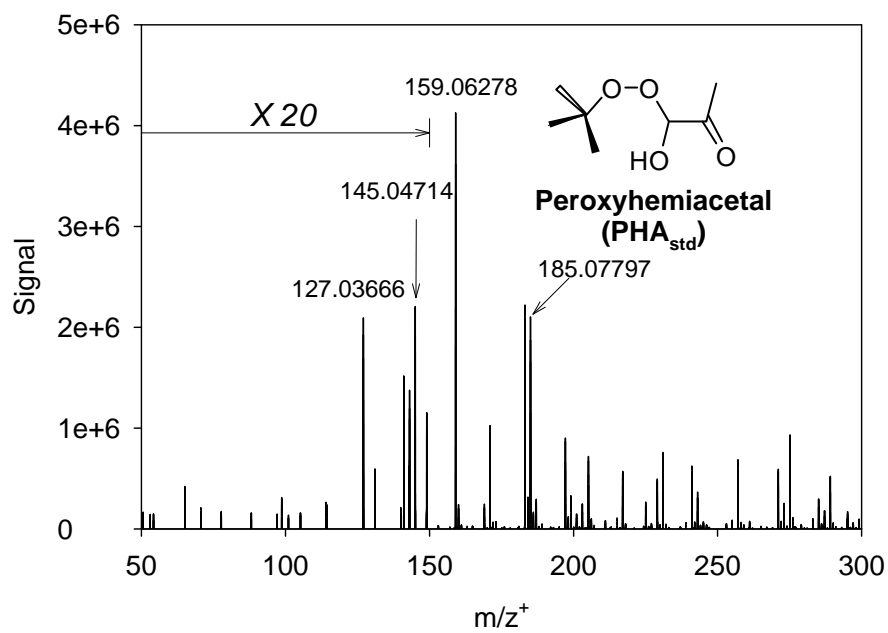
1

2 FIGURE 3. A full FTICR-MS spectrum for the standard solution of methylglyoxal (10 mM)
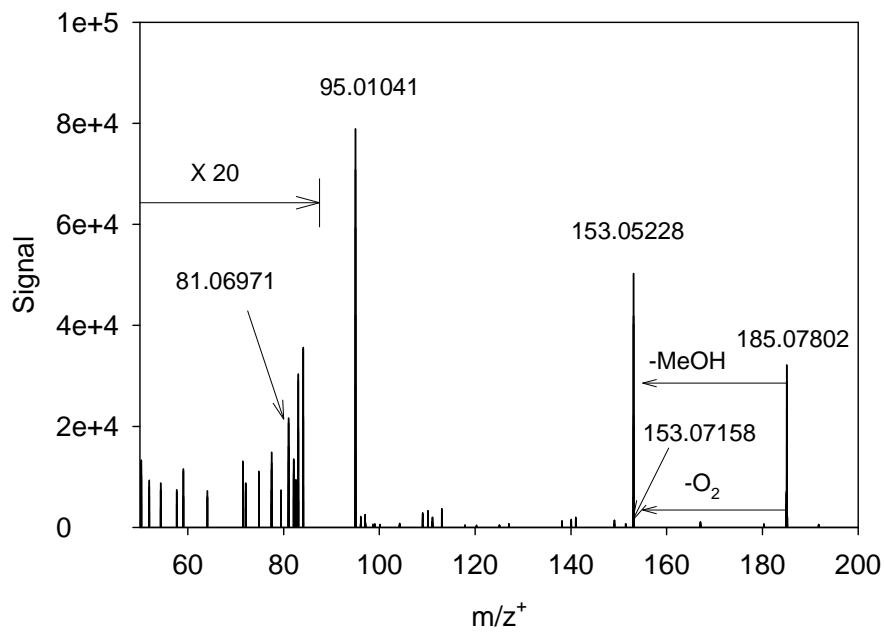
3 and tert-butyl hydroperoxide (10 mM) in the positive mode.

4

5

1

2　FIGURE 4. FTICR-MS/MS for m/z$^+$ 159 (methylglyoxal).

3

1

2

3   FIGURE 5. FTICR-MS/MS for m/z$^+$ 185 (PHA$_{std}$).

4

5
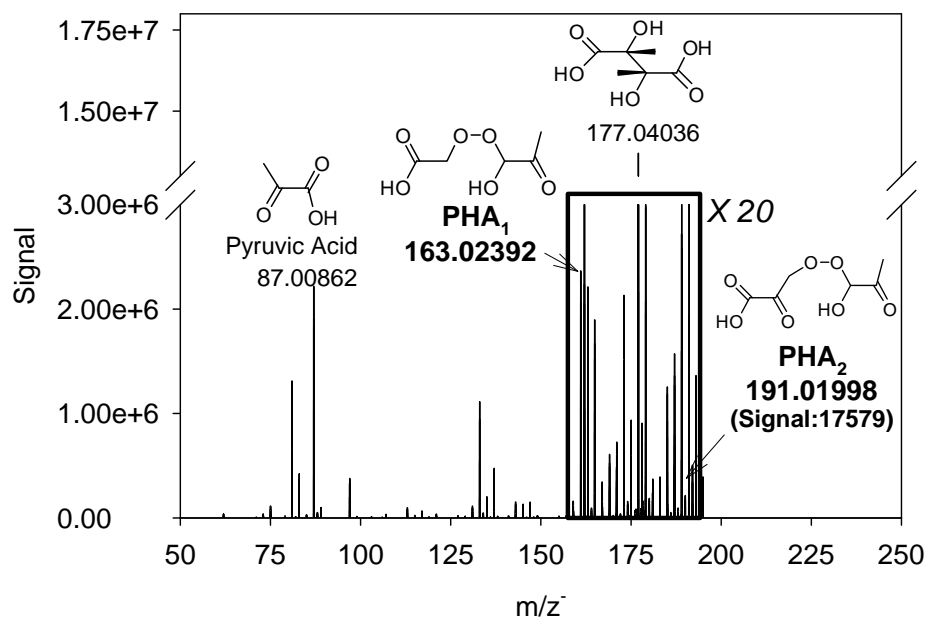
FIGURE 6. A full FTICR-MS spectrum for products of 1-hr aqueous photooxidation of methylglyoxal in the negative mode.
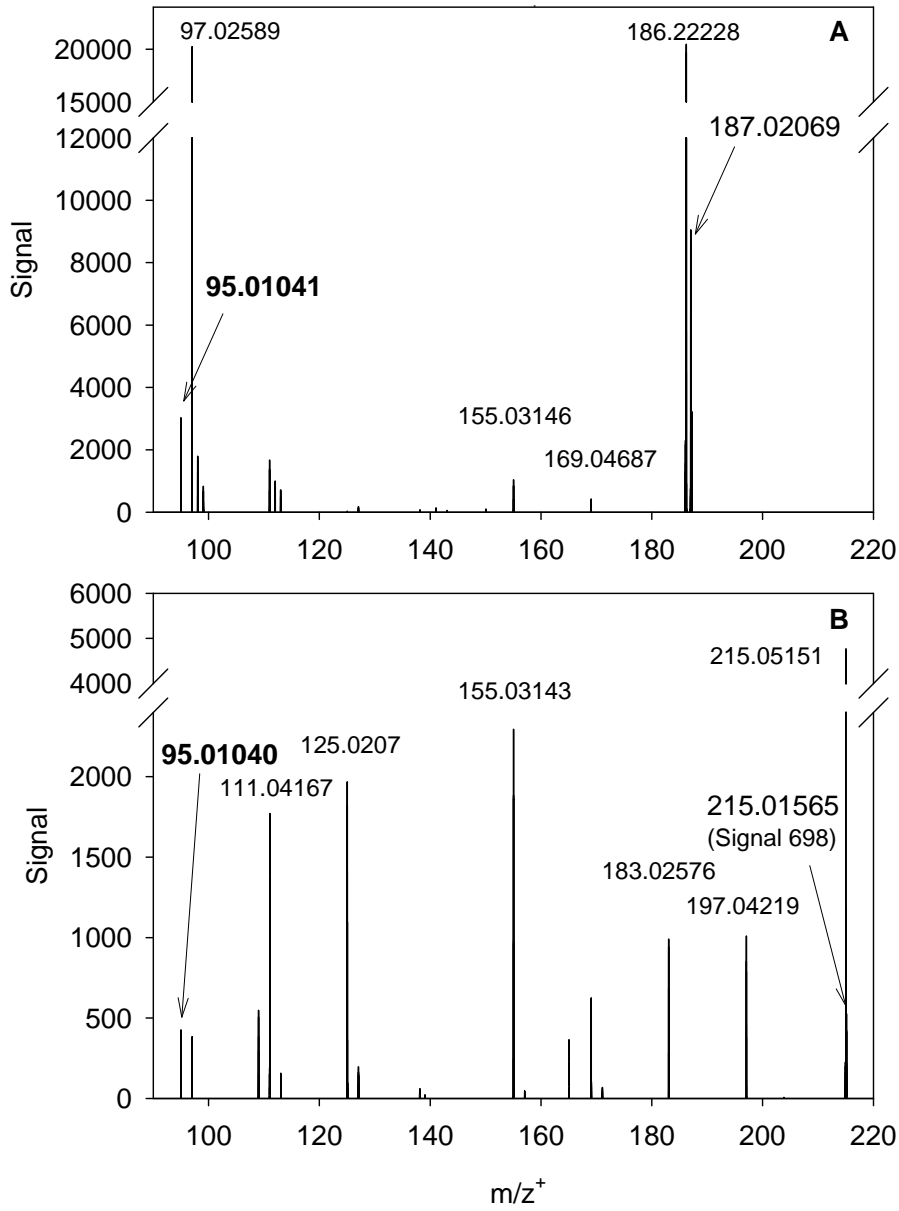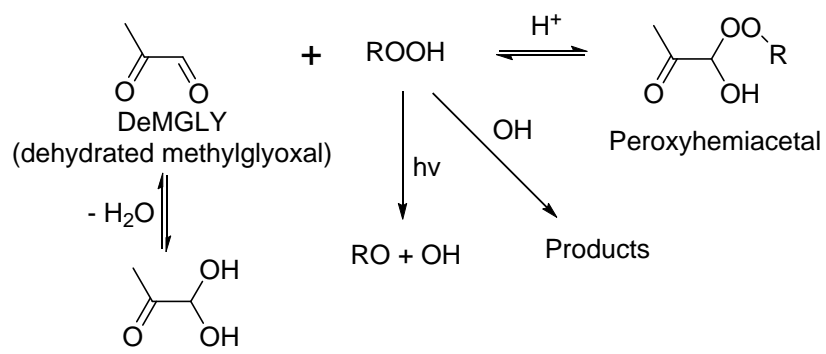
1
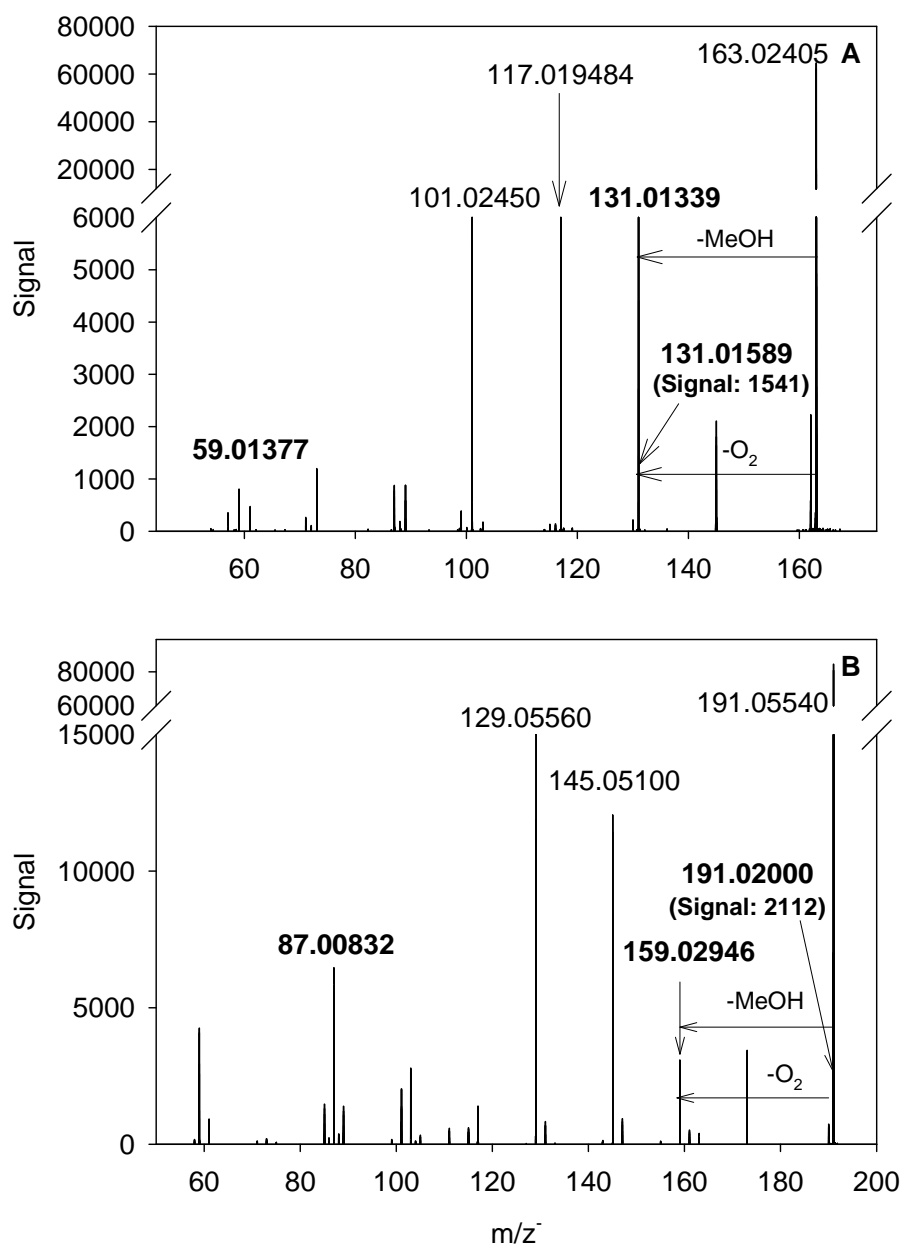
2

3 FIGURE 7. FTICR-MS/MS for m/z⁻ 163 for PHA₁ (**A**) and m/z⁻ 191 PHA₂ (**B**).

4

1

2 **FIGURE 8.** FTICR-MS/MS for m/z$^+$ 187 for PHA$_1$ (**A**) and m/z$^+$ 215 for PHA$_2$ (**B**).
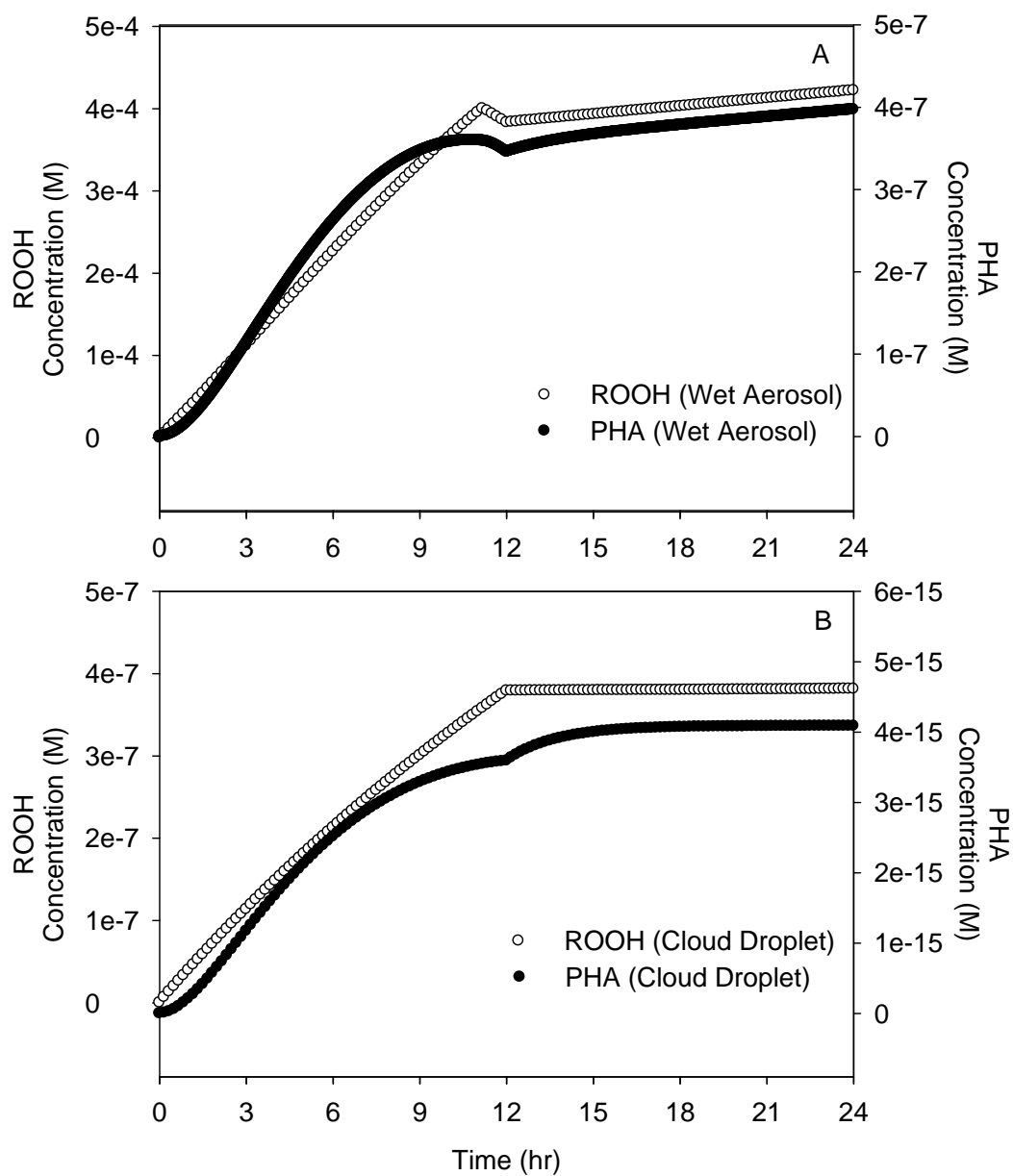
3

4

FIGURE 9. Peroxyhemiacetal formation

1

2   FIGURE 10. The atmospheric simulated concentrations of ROOH (organic peroxides) and

3   PHA (peroxyhemiacetals) in wet aerosols (**A**) and cloud droplets (**B**) during 24 hrs. The first

4   12 hrs are daytime.

5